STATUS OF MODIS LAI-FPAR ALGORITHM

Boston University
Y. Zhang
Y. Tian
N. Shabanov
R. Myneni
Y. Knyazikhin

University of Montana
P. Votava
J. Glassy
S. Running

MODIS SCIENCE TEAM MEETING

JUNE 24-26, 1998

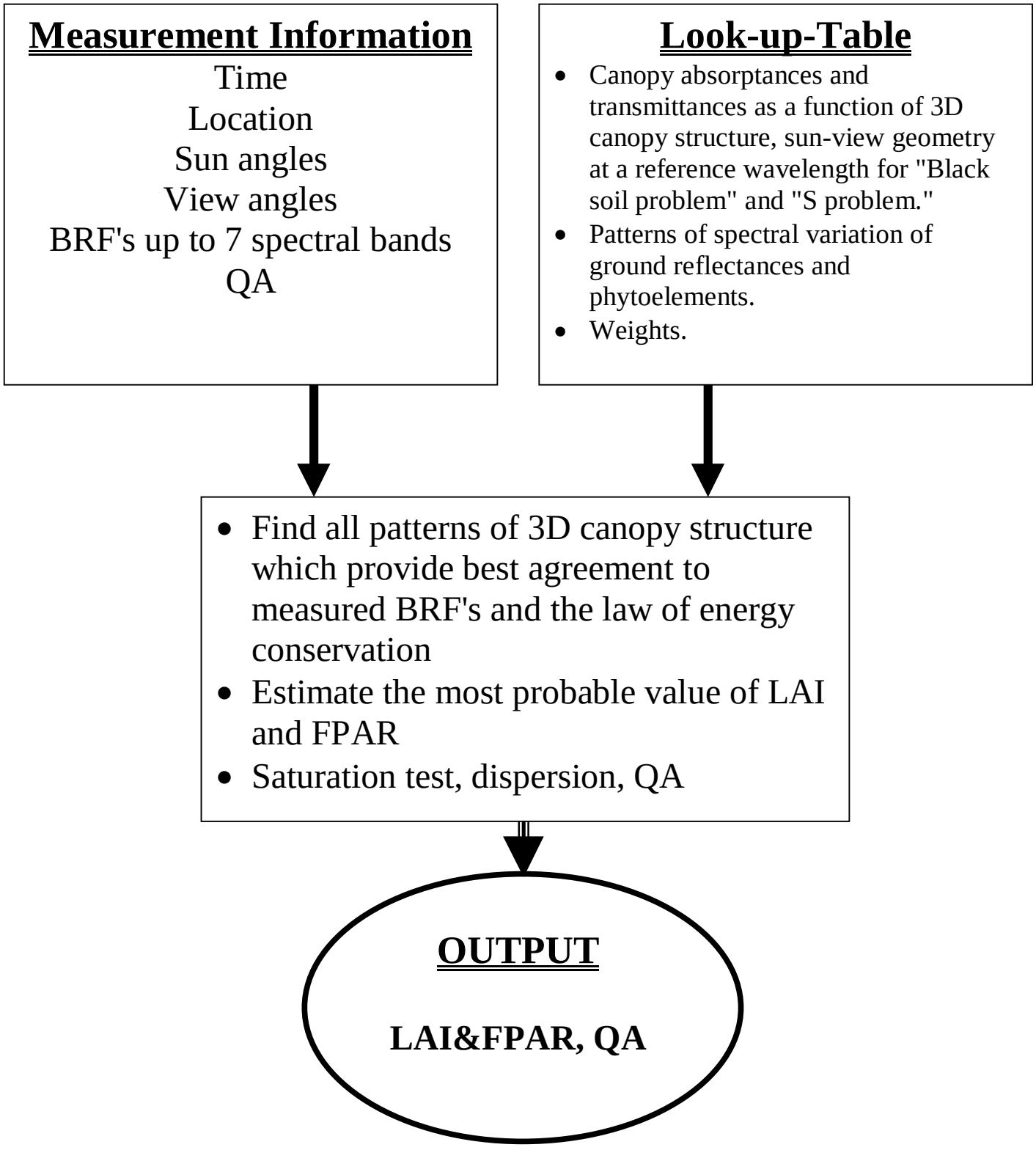
Measurement Information
Time
Location
Sun angles
View angles
BRF's up to 7 spectral bands
QA
Look-up-Table
Canopy absorptances and transmittances as a function of 3D canopy structure, sun-view geometry at a reference wavelength for "Black soil problem" and "S problem."
Patterns of spectral variation of ground reflectances and phytoelements.
Weights.
Find all patterns of 3D canopy structure which provide best agreement to measured BRF's and the law of energy conservation
Estimate the most probable value of LAI and FPAR
Saturation test, dispersion, QA
OUTPUT
LAI&FPAR, QA

Contents of the Look-up-Table

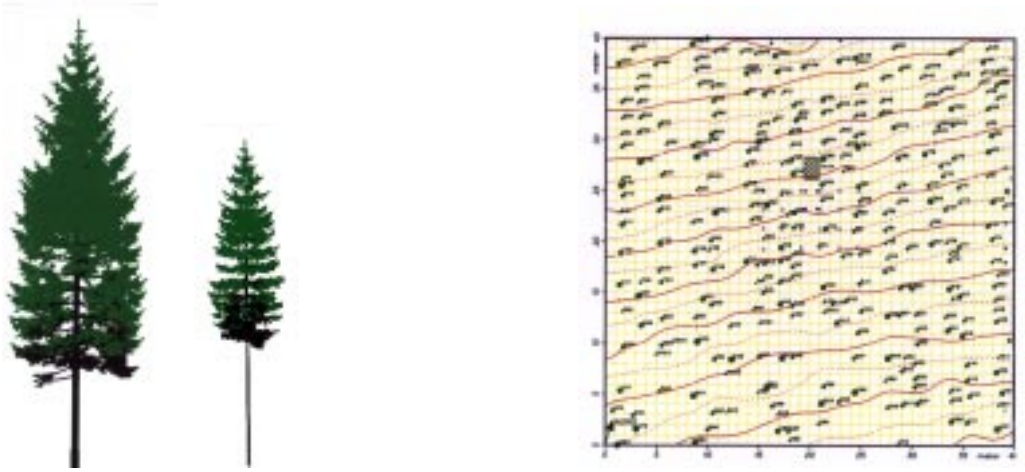

A. Patterns of the architecture of individual trees (left) and the entire canopy (right).

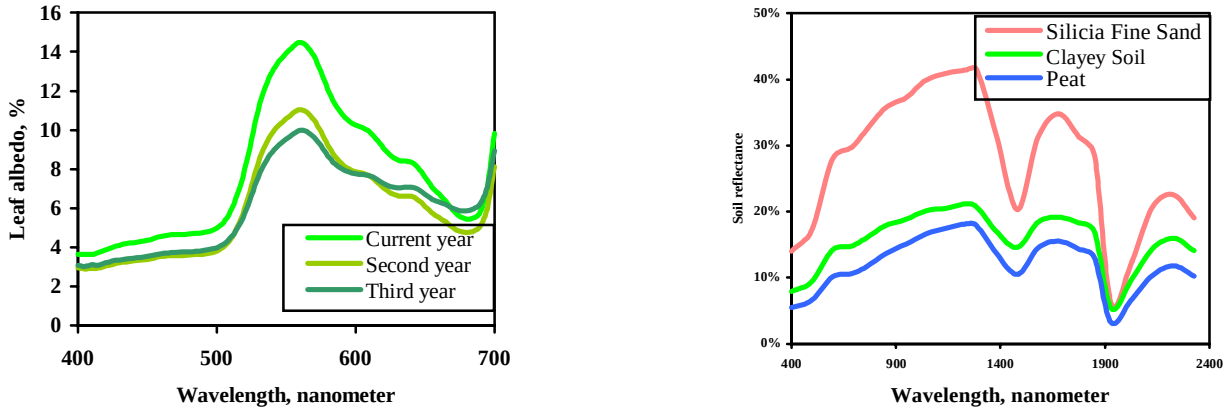

B. Patterns of spectral leaf albedos and soil reflectances.

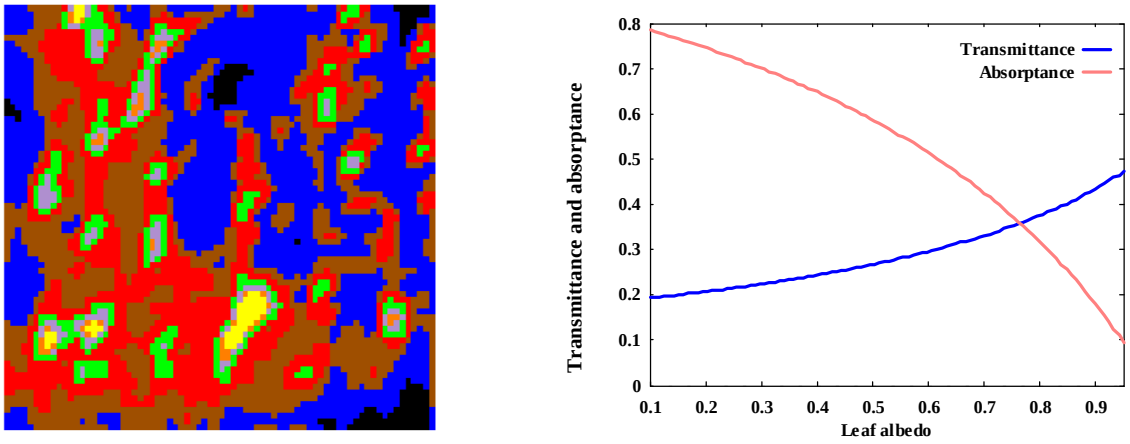

C. Three-dimensional distribution of canopy transmittance. Mean canopy transmittance (over ground surface) and absorptance (over canopy) as a function of leaf albedo.

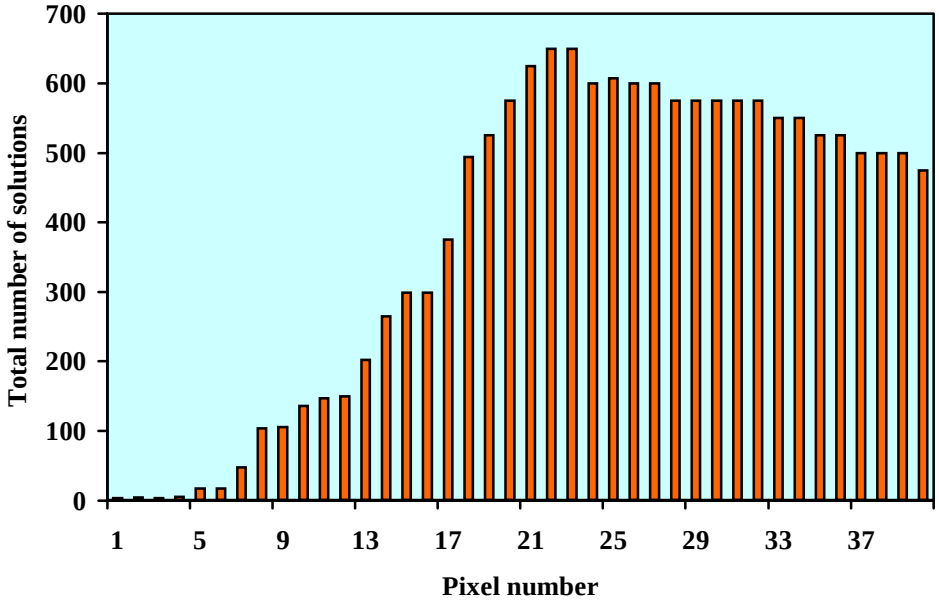

For each pixel, the algorithm aims at solving the following inverse problem: given biome type, spectral and, in case of MISR data, angular signature of pixel leaving radiance, and their uncertainties, find the leaf area index of this pixel and a fraction of photosynthetically active radiation absorbed by vegetation in this pixel. However this problem allows multiple solutions: some combinations of canopy structure and soil type may results in the same spectral set of measured canopy reflectances. This figure demonstrates number of solutions for 40 pixels of different sets of measured spectral reflectances.

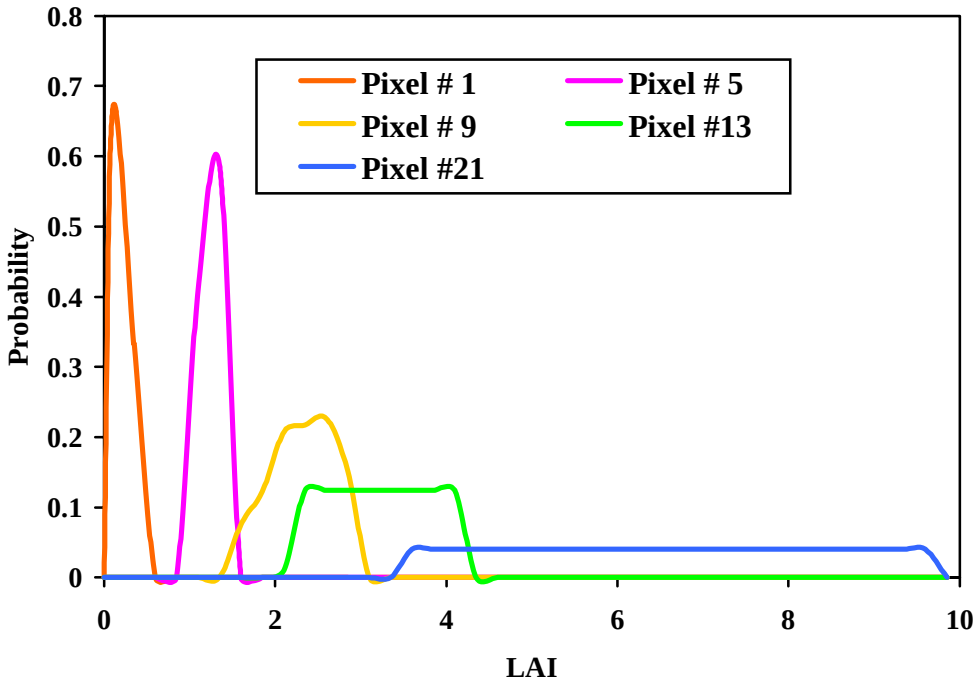

We use the measure theory to evaluate probabilities of various LAI values of a pixel analyzed using the set of all possible solutions. This plot demonstrates the distributions of LAI values for 5 pixels from the above figure. The most probable value of LAI and FPAR can now be evaluated as a mathematical expectation of LAI and FPAR over estimated LAI distribution function.

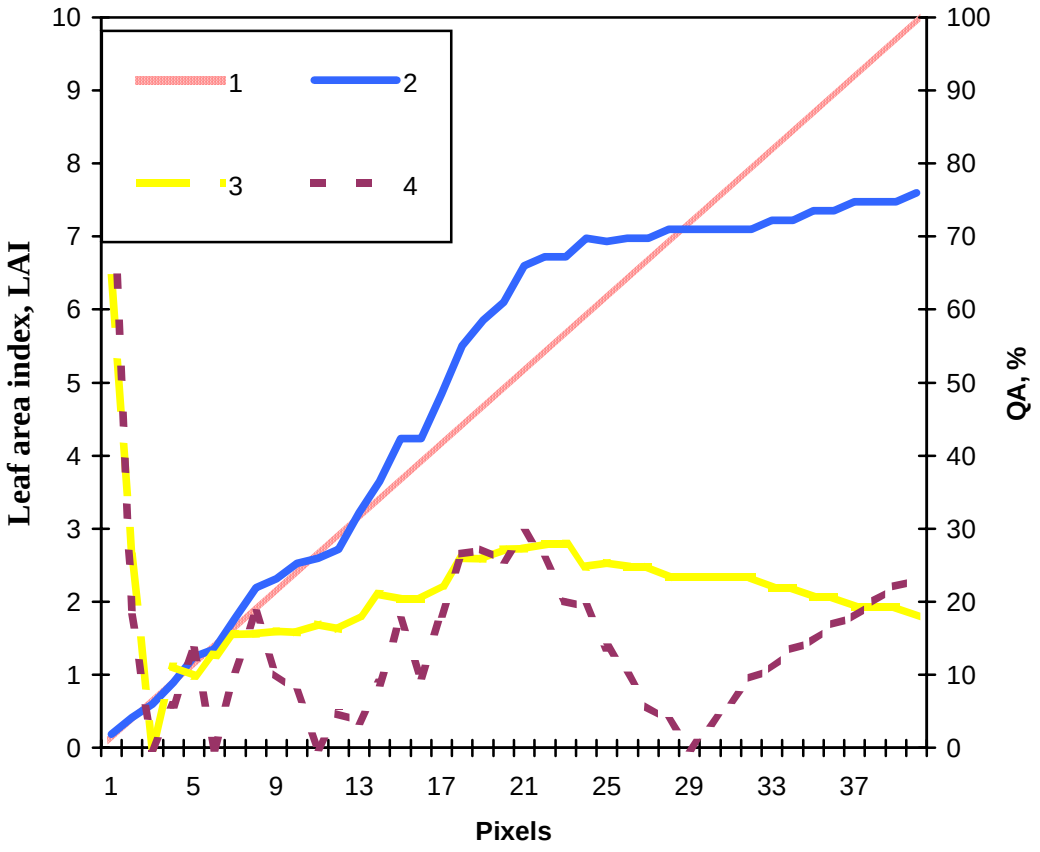

Comparison of the retrieved and exact solutions of the inverse problem for 40 simulated pixels. 1: exact solutions; 2: retrieved solutions; 3: variance; 4: relative accuracy. Input uncertainties were 20%.

Distribution of pixels in RED-NIR plane

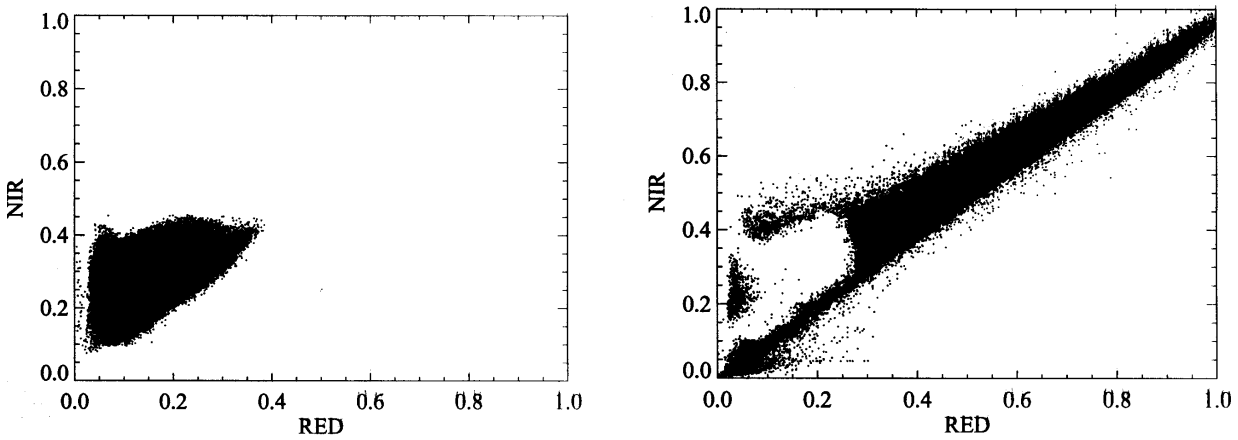

These plots demonstrate distribution of pixels with respect to their reflectances at near-infrared and red wavelengths derived from the SeaFIWS data set (September 22, 1997). The left plot shows all pixel for which the utilization of our algorithm was successful. The right plot contains those pixels for which the algorithm failed. The algorithm was applied to every pixel marked in this data set as biome 1 (Grasses and Cereal Crops). Number of successful pixels makes up 70% in this example.

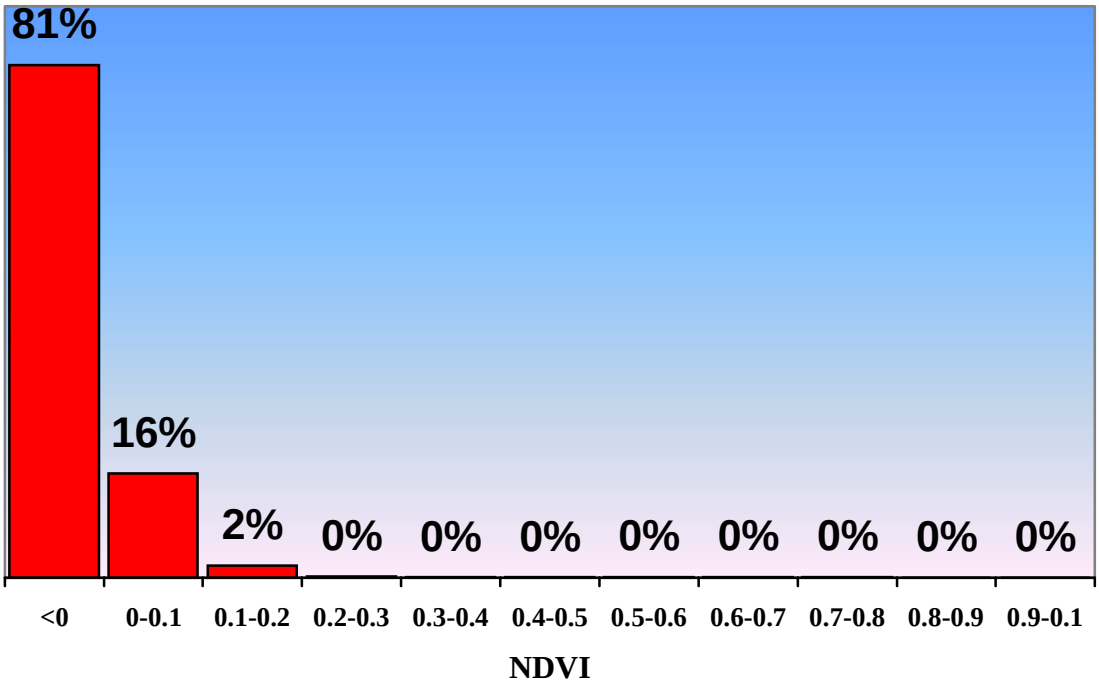

Distribution of "unsuccessful" pixels with respect to the NDVI values. One can see that unsuccessful pixels are mainly concentrated in the plot area for which value of NDVI is less than 0.1. Thus our algorithm does not produce values of LAI and FPAR in case when the pixels are non-vegetated or data are corrupted due clouds or atmosphere effect.

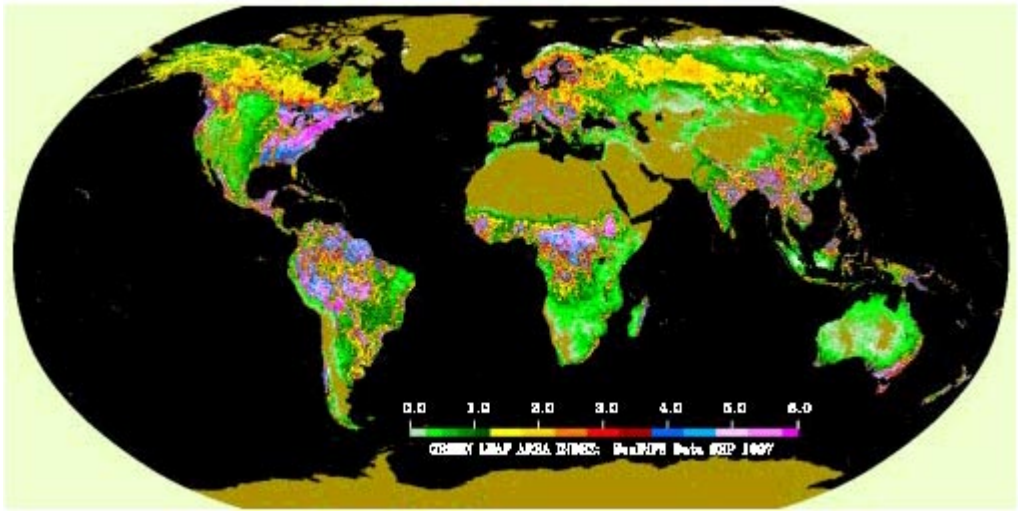

a)

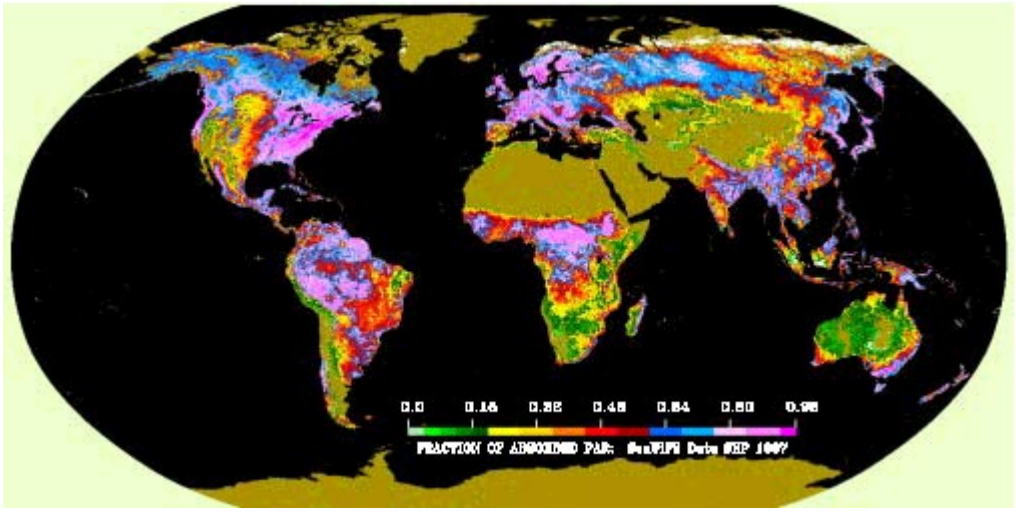

b)

Global LAI [panel (a)] and FPAR [panel (b)] in September - October 1997 derived from SeaWiFs (Sea-viewing Wide Field-of-view Sensor) data. This data set includes daily atmosphere corrected surface reflectances at 8 shortwave spectral bands. Surface reflectances at red (670 nm) and near-infrared (865 nm) at 8 kilometer resolution were used. The algorithm was applied to daily surface reflectance data for all days from 18 Sep to 12 Oct 1997. For each pixel, LAI and FPAR values corresponding to the maximum NDVI during this period are shown in these panels.

SeaWIFS data set

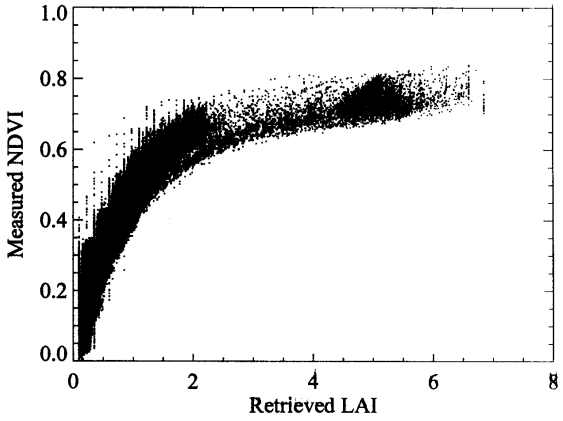

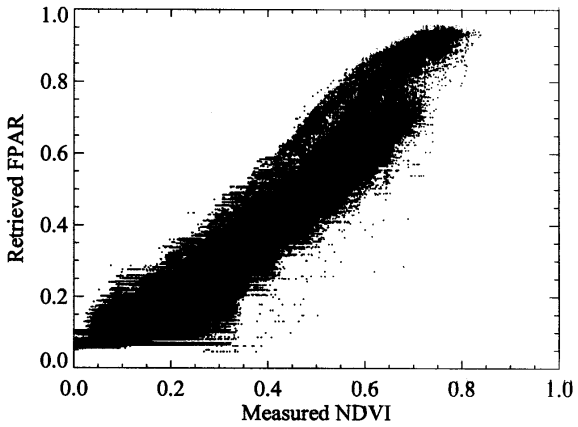

LASUR data set

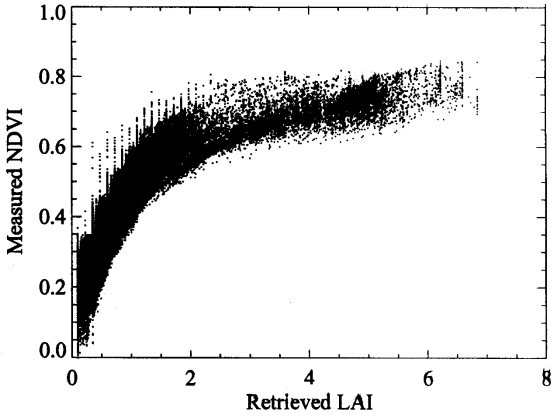

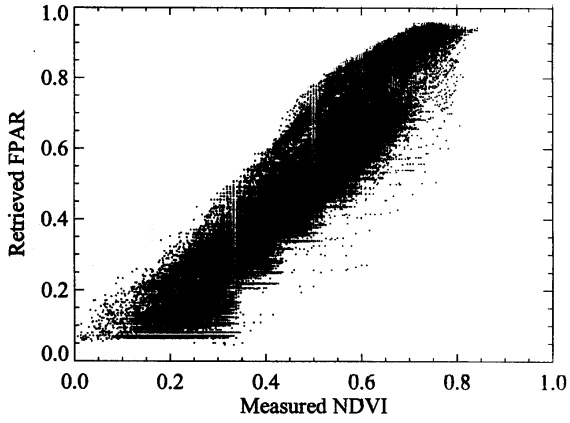

The Normalized Difference Vegetation Index (NDVI) is the ratio of the difference between canopy reflectances at near-infrared and red wavelengths to their sum. This plot demonstrates NDVI-LAI and FPAR-NDVI relationships for biome 1 (Grasses and Cereal Crops) estimated with our algorithm applied to the SeaFIWS (top, September 22, 1997) and LASUR (bottom, July 10, 1997) data sets. These relationships are similar to those reported in the literature.

The success index* for various combinations of spectral bands used to retrieve LAI and FPAR

Spectral bands used				Success index, %
NIR	Red	Blue	Green	
x	x			96.8
x	x		x	95.0
	x		x	94.9
x			x	94.8
x		x		86.5
x		x	x	77.8
x	x	x	x	77.8
x	x	x		75.2

*The success index was calculated here as the ratio of number of successful pixels to the total number of pixels for which NDVI>0.1. Values of the index are expressed in %.

The use of the blue band results in poor retrievals. The following arguments can be presented. The optical properties of foliage elements at blue and red wavelengths are similar. Thus, the surface reflectances are comparable in magnitude. However, atmospheric effect at blue band is much stronger than at the red band. As a result, the uncertainties in the atmospherically corrected BRF's data are greater at blue than at red band. In prototyping the LAI/FPAR, product we assumed that uncertainties in LASUR and SeAWiFS data sets were wavelength independent. Thus, the algorithm processes the blue and red BRF's with equal weight. The use of blue BRF, therefore, results in poorer retrievals. Holding uncertainties constant, all combinations of spectral bands without the blue provide better results than ones including the blue band.

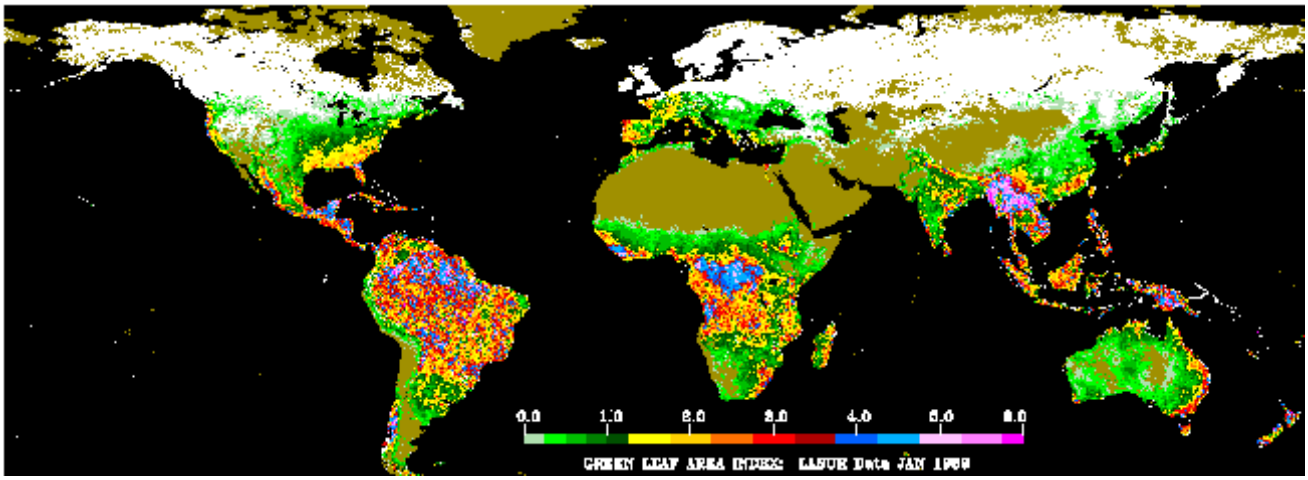

a)

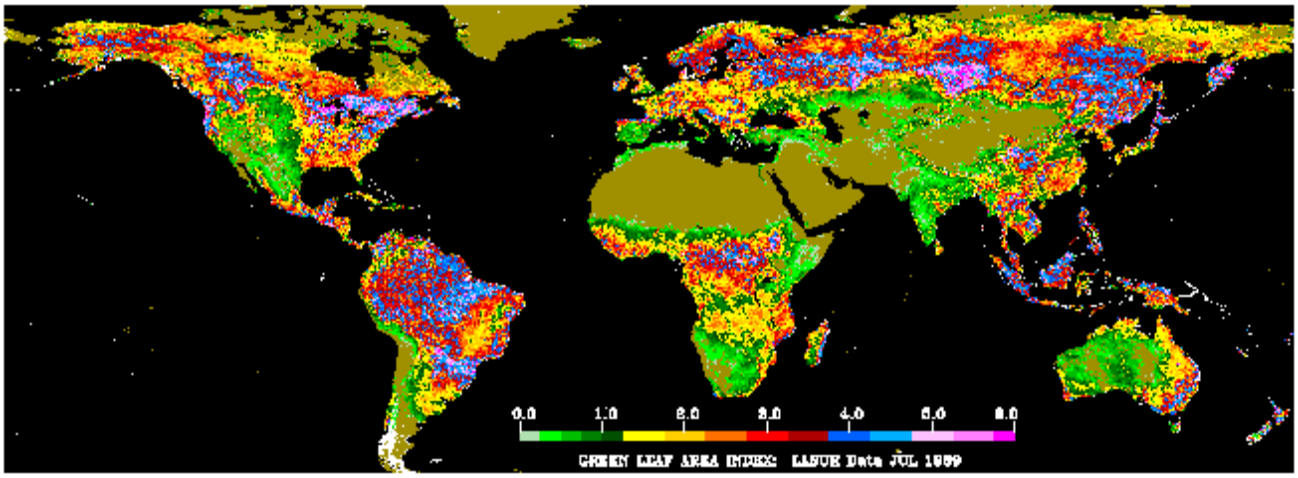

b)

Global LAI derived from LASUR (LAnd SUrface Reflectance) data. This data set includes atmospherically corrected surface reflectances in the red and near-infrared channels of the Advanced Very High Resolution Radiometer (AVHRR) at global scale (1/7,1, and 5 square degree resolution; one week temporal resolution) for 1989 and 1990. The algorithm was applied to the weekly surface reflectance data (8 km) for 4 weeks in January and for 4 weeks in July. These panels show the color-coded images of global LAI in January (a) and in July (b) composited based on maximum NDVI during those four weeks.

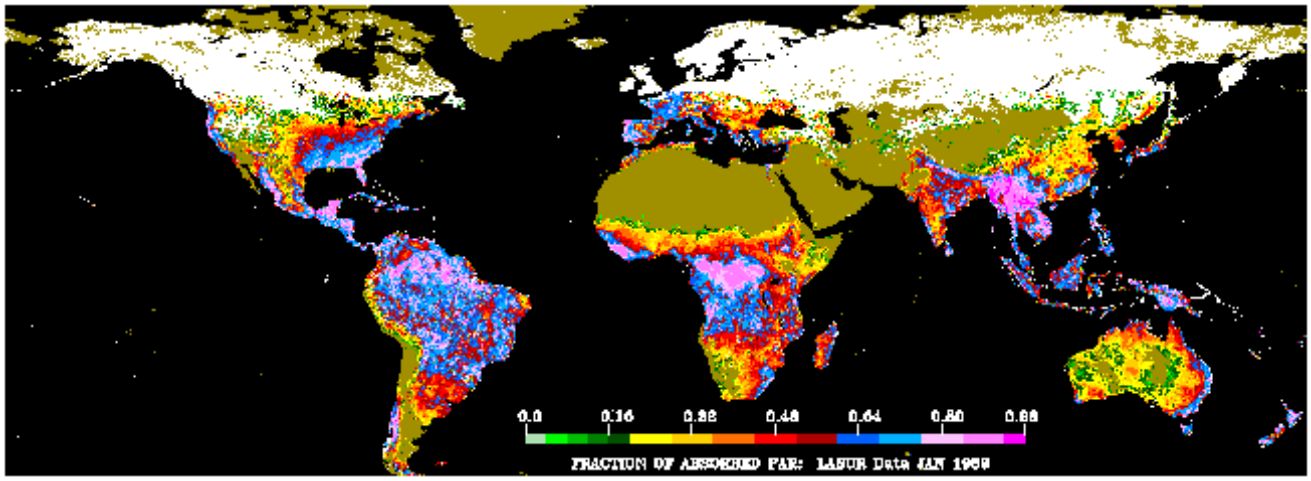

a)

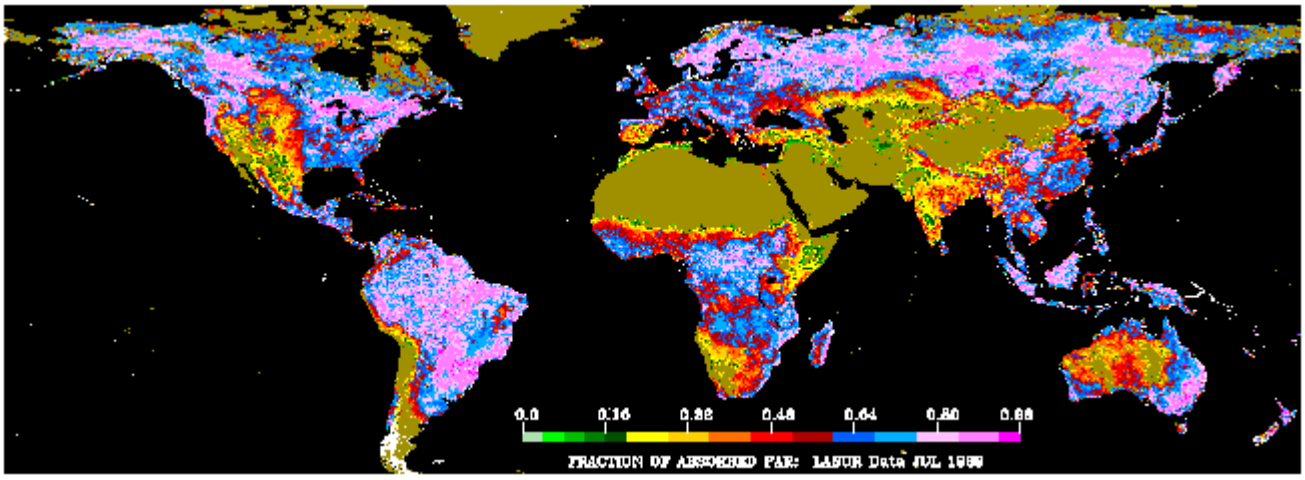

b)

Global FPAR derived from LASUR data. The algorithm was applied to the weekly surface reflectance data (8 km) for 4 weeks in January and for 4 weeks in July. These panels show the color-coded images of global FPAR in January (a) and in July (b) composited based on maximum NDVI during those four weeks.

Regression curves.

The measure theory is used to establish relationships between the surface reflectances, uncertainties in their retrieval, canopy structure and optical properties of vegetation elements (leaves, stems, etc.) and soil. This theory is the mathematical foundation of the modern probability theory. It allows us to treat values of NDVI, LAI and FPAR as random variables. Statistical techniques, therefore, can be utilized to analyze relationships between NDVI, LAI and FPAR.

Definition. Two curves $x(y)=E(X \mid Y=y)$ and $y(x)=E(Y \mid X=y)$ defined in the (x,y)-*plane* are called the regression curves of X with respect to Y and of Y with respect to X, respectively. Here, X and Y are random variables; $E(X \mid Y=y)$ is expectation of X under the condition that Y has taken the value y. The regression curve has the following interpretation: the best possible prediction of X given a realized value y_0 of Y is $x(y_0)$. The regression function $x(y)$ minimizes the expected squared error of the prediction of X on the basis of value of y, and $y(x)$ can be interpreted similarly.

The regression curve can be used to analyze the LAI-NDVI and NDVI-FPAR relationships. Let X, Y, and Z be random variables of LAI, NDVI and FPAR values. We denote the regression curves of LAI with respect to NDVI and of NDVI with respect to LAI by $x(z)$ and $z(x)$ respectively. Similarly, $y(z)$ and $z(y)$ denote the best possible prediction of FPAR given a realized value z of NDVI and the best possible prediction of NDVI given a realized value z of FPAR.

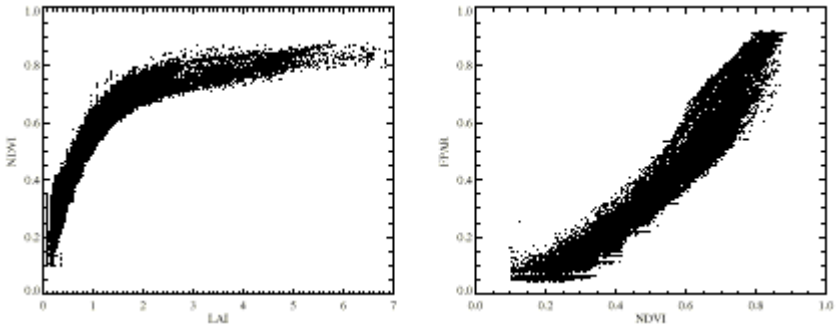

Realizations of X, Y and Z with respect to retrieved values of LAI and LASUR NDVI field [left panel] and to retrieved values of FPAR and LASUR NDVI field [right panel]. These spaces of realizations of X, Y and Z are used to derive the best possible prediction of LAI, FPAR and NDVI values.

Regression curves derived from the LASUR data

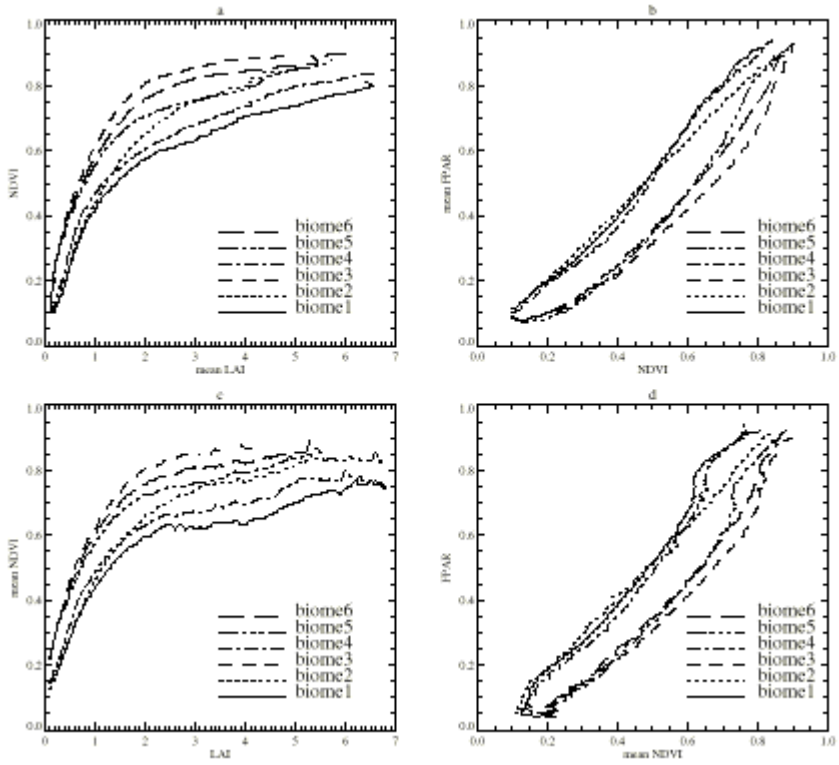

The regressions curves $x(z)$, $z(x)$, $y(z)$ and $z(y)$ for 6 biomes (Grasses and Cereal Crops; Shrubs, Broadleaf Crops; Savannas; Broadleaf Forests; Needleleaf Forests). The surface reflectance was treated as a biome dependent random variable. The LASUR data was taken as the set of realizations of canopy reflectances. The LAI/FPAR algorithm was applied to this data set in order to evaluate the set of realizations of LAI and FPAR values. Panels (a) and (b): the best possible prediction of LAI and FPAR given a realized value y of NDVI. Panels (c) and (d): the best possible prediction of NDVI given realized values x and z of LAI and FPAR.

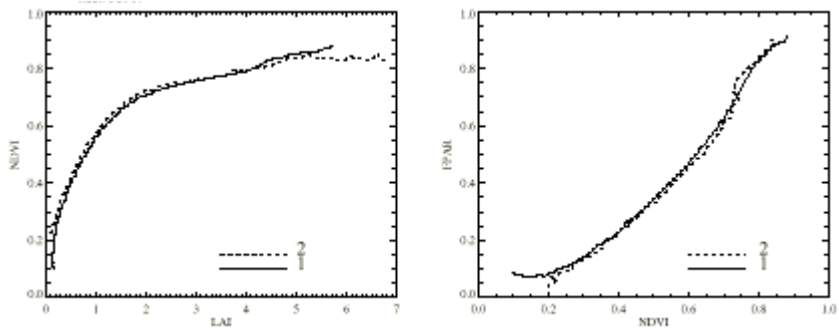

Regression curves for biome 5 (Broadleaf Forests). Left panel: the best possible prediction of LAI, $x(y)$ [curve 1], given a realized value y of NDVI, and the best possible prediction of NDVI, $y(x)$ [curve 2], given a realized value x of LAI. The regression curves $z(y)$ [curve 1] and $y(z)$ [curve 2] are shown in the right panel.

Comparison of synthetic canopy reflectances with the LASUR and SeaWiFS data sets

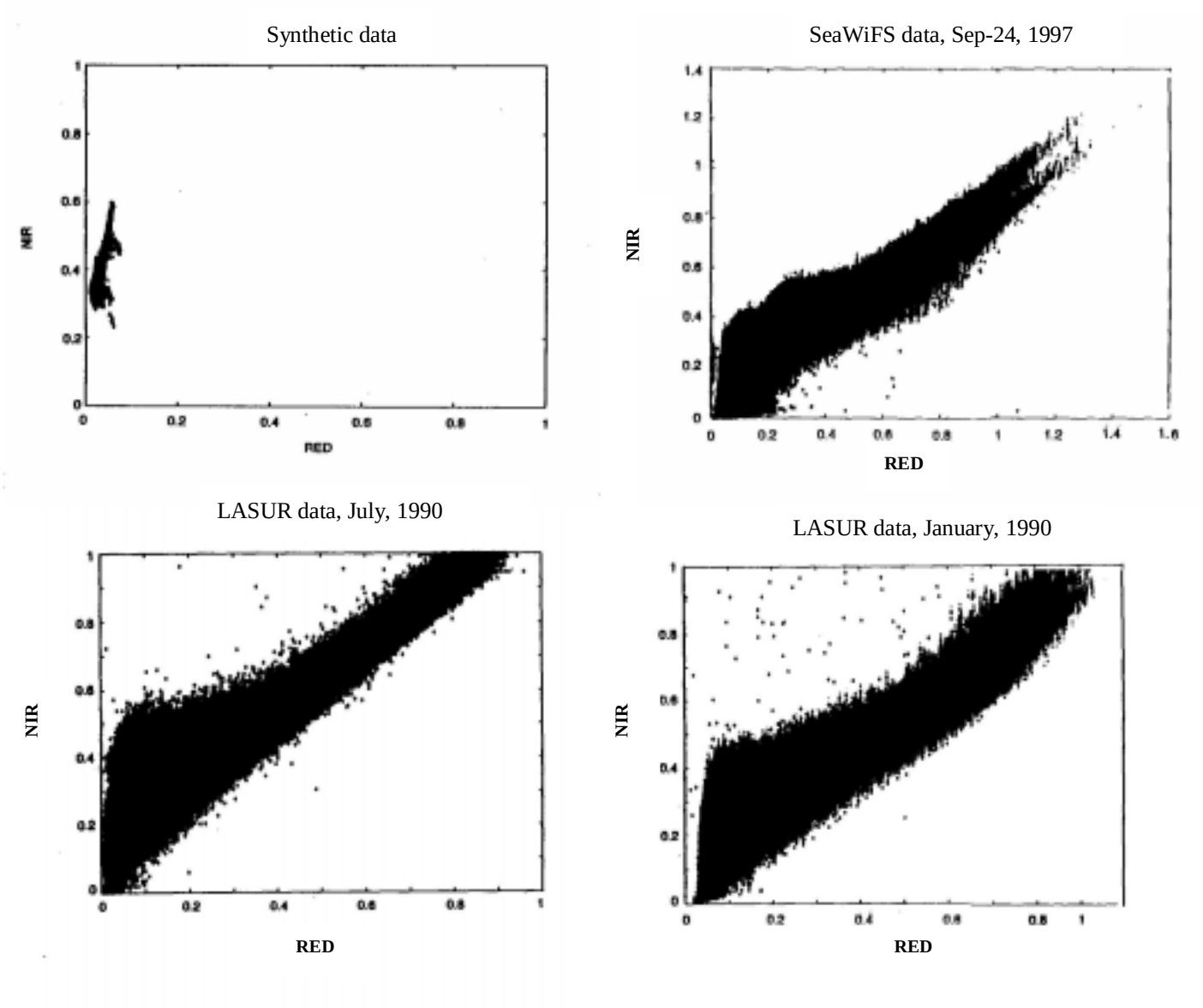

Distribution of pixels with respect to their reflectances at near-infrared and red wavelengths derived from the synthetic, LASUR and SeaWIFS data sets.

Table. Intervals which include 90% of all values of NDVI, Simple Ratio (SM), canopy reflectances at red (RED) and near-infrared (NIR) wavelengths for the synthetic, LASUR and SeaWiFS data sets.

	Synthetic data	*LASUR (July)*	*LASUR (January)*	*SeaWiFS (September-October*
NDVI	[0.68, 0.92]	[-0.04, 0.8]	[-0.04, 0.8]	[-0.2; 0.6]
SM	[10.0, 26.4]	[0.0, 11.6]	[0.0, 11.6]	[0.2, 4.0]
RED	[0.03, 0.046]	[0.03, 0.5]	[0.03, 0.43]	[0.04, 0.89]
NIR	[0.28, 0.58]	[0.1, 0.9]	[0.1, 1.0]	[0.1, 0.9]

Lessons learned

1. The fundamental physical principle, the law of energy conservation, is the basis of our LAI/FPAR algorithm. A key idea in incorporating this law in the algorithm is the use of the critical eigenvalue to relate canopy structure and optical properties of phytoelements. The critical eigenvalue and the unique positive eigenvector corresponding to this eigenvalue express the law of energy conservation in a compact form. Although the use of such an approach was theoretically, no evidence of its functionality was presented. Results from prototyping of the LAI/FPAR product demonstrate not only its ability to produce the global LAI and FPAR fields but also to use all information provided by MODIS instrument.

2. The algorithm mainly fails if a pixel is non-vegetated or data is corrupted due to clouds or atmospheric effect.

3. The algorithm can use all spectral information (bands 1 through 7) of the MODIS instrument. However, the quality of the retrievals can not be better than the quality of the worst spectral BRF, if uncertainties in spectral BRF's are not available. Evaluation of the uncertainties in atmospherically corrected surface reflectances is critical to improve the quality of the LAI/FPAR product, and to realize the full potential of the MODIS and MISR instruments.

4. If uncertainties in atmospherically corrected surface reflectances are not available, the use of NIR, Red, and Green spectral bands are optimal.

A theoretical basis of the algorithm is presented in the following articles submitted for publication in the EOS-AM1 special issue of the JGR:

Knyazikhin, Yu., J.V., Martonchik, R.B. Myneni, D.J. Diner, and S. Running, Synergistic algorithm for estimating vegetation canopy leaf area index and fraction of absorbed photosynthetically active radiation from MODIS and MISR, *EOS-AM special issue of J. Geophys. Res.*, 1997a (submitted for publication).

Knyazikhin, Yu., J.V. Martonchik, D.J.Diner, R.B. Myneni, M.M. Verstraete, B.Pinty, and N. Gobron, Estimation of vegetation canopy leaf area index and fraction of absorbed photosynthetically active radiation from MISR data, *EOS-AM special issue of J. Geophys. Res.*, 1997b (submitted for publication).

These articles can be downloaded as:

ftp crsa.bu.edu
login anonymous
Password enter your e-mail address
cd pub/jknjazi/Papers/
mget mget MISR_LAI_FPAR.pdf Synergistic.pdf